J Stat Phys (2010) 141: 1093–1103
DOI 10.1007/s10955-010-0088-4

# Transport Equation Evaluation of Coupled Continuous Time Random Walks

**Harvey Scher · Karen Willbrand · Brian Berkowitz**

Received: 26 August 2010 / Accepted: 1 November 2010 / Published online: 9 November 2010


**Abstract** The transport behavior of a migrating particle in a disordered medium is exhibited in the solution of a transport equation derived from a coupled continuous time random walk (CTRW). A core aspect of CTRW is the spectrum of transitions in displacement $\mathbf{s}$ and time $t$, $\psi(\mathbf{s}, t)$, that characterizes the disordered system, which determine the transport. In many applications the CTRW approach has successfully accounted for the anomalous or non-Fickian nature of the particle plume propagation based on a power-law dependence $\psi(t)$ in a decoupled $p(\mathbf{s})\psi(t)$ approximation to $\psi(\mathbf{s}, t)$. For example, this power-law dependence in $t$ derives from the complex Darcy flow fields in geological formations. Recently, the fully coupled CTRW was analyzed using a particle tracking approach, demonstrating that the decoupled approximation is valid only for a compact distribution of $s$. In this paper we solve the nonlocal-in-time transport equation with a $\psi(\mathbf{s}, t)$ containing a power-law dependence in both $s$ (a Lévy-like distribution) and $t$, which necessitates the strong $\mathbf{s}, t$ coupling. We show enhanced transport behavior (relative to the plume propagation behavior reported in the literature) that derives from the rare large displacements in $s$ (limited by the transition $t$). The interplay between the two coupled power laws is clearly shown in the changes in the breakthrough curves in the arrival times, dispersion and dependence on the velocity ($v = s/t$) distribution. Similar enhancements are exhibited in the particle tracking results.

**Keywords** Anomalous transport · Non-Fickian transport · Random walks · Disordered media

H. Scher · K. Willbrand · B. Berkowitz (✉)
Department of Environmental Sciences and Energy Research, Weizmann Institute of Science, Rehovot, Israel
e-mail: brian.berkowitz@weizmann.ac.il

H. Scher
e-mail: harvey.scher@weizmann.ac.il

K. Willbrand
e-mail: karen.willbrand@weizmann.ac.il

## 1 Introduction

An intrinsic feature of a disordered system is the broad spectrum of transfer rates encountered by a migrating particle [6]. These rates could involve charge transfer between molecular sites in a doped polymer [25] or displacements in a complex Darcy flow field in a geological formation [4]. This type of spectrum typically contains statistically rare transfers that can have a large effect on particle transport, leading to anomalous (or non-Fickian) dispersion. Therefore theoretical modeling of this phenomenon must incorporate the entire spectrum of transfer rates.

We have used the approach of a continuous time random walk (CTRW) and placed at its core a spectrum represented as a joint probability density $\psi(\mathbf{s}, t)$ of random space displacements $\mathbf{s}$ and transfer times $t$ [4]. The use of the CTRW to model chemical plumes migrating in the complex saturated flow fields of geological formations, containing heterogeneities over multiple length scales [11, 13, 17], has utilized the time spectrum in a decoupled mode $\psi(\mathbf{s}, t) = p(\mathbf{s})\psi(t)$. Here $\psi(t)$ contains a power law region as the source of the anomalous transport behavior, especially the significant effect of infrequent large time transitions, e.g., due to an encounter with a low velocity zone.

The application of the CTRW involves a nonlocal-in-time integro-differential transport equation (referred to as the CTRW partial differential equation, CTRW pde). The derivation of this equation is a Fokker-Planck expansion of a Generalized Master Equation, whose origin is the ensemble average of the Master Equation [23] which contains all of the aforementioned transfer rates, denoted $w(\mathbf{s}, \mathbf{s}')$ for a transition between $\mathbf{s}$ and $\mathbf{s}'$ [2]. The solution of this CTRW pde for the decoupled $p(\mathbf{s})\psi(t)$ has enabled an accounting of a wide range of unusual transport phenomena in experimental observations in the laboratory and at the field scale [4]. In this context, numerical simulations of a spectrum of local transfers, derived from local displacements and velocities, have been used to obtain $\psi(\mathbf{s}, t)$ on the field scale [10], the pore scale [5], in two-dimensional random fracture networks [2] and in idealized conductivity fields [12, 26].

The CTRW pde with the decoupled $p(\mathbf{s})\psi(t)$ has the form of a convolution of the advection-dispersion equation with a memory function. But the nonlocal-in-time equation with a fully coupled $\psi(\mathbf{s}, t)$ has a more general form and can admit to a greater range of chemical plume propagation. The CTRW framework generally emphasizes the significant effect of statistically rare large time transitions, e.g., due to an encounter with a low velocity zone (i.e., a high inverse velocity $\xi \equiv 1/v$, where $v = |\mathbf{v}|$ is the absolute particle velocity). This encounter is enhanced if the $\xi$-dependence of the velocity distribution function $\Phi(\xi)$ is a power-law tail. However, another possibility for a significant statistically rare event is a large displacement (compared to the median displacement) if a system, e.g., a random fracture network, has a power-law $s$-distribution. The contribution of such displacements to the plume transport at a given time would depend on a sampling of the higher velocities, i.e., the small $\xi$ region of $\Phi(\xi)$. These types of events suggest the need for a coupled $\psi(\mathbf{s}, t)$ between a power law in time and a Lévy [19, 20] walk in space [16, 18, 21]. As noted above, the decoupled form has been effective in many applications to transport in porous and fractured media. The fully coupled solutions of the CTRW pde that we develop here represent an additional tool to use in systems to be explored that have extensive spatial correlations.

The purpose of this paper is to present a solution of this CTRW pde, which is the first one for a fully coupled $\psi(\mathbf{s}, t)$, and demonstrate the resulting enhanced transport behavior. This behavior is most significant when the $\psi(\mathbf{s}, t)$ contains, in addition to an algebraic (power-law) $t$-dependence, a power-law dependence on $s$ (a Lévy-like distribution, but limited by the finite velocity $v = s/t$ at each step). We are, basically, exploring the effect of

the rare event of a large spatial displacement in the context of the wide spectrum of transition times. The interplay of the power-law distributions in spatial displacements and in time are displayed in our solutions for the breakthrough curves. The broader the $s$-tail, the more extended the dispersion due to the algebraic $t$-dependence and the greater the change in the early time arrivals as shown in the breakthrough curves of concentration vs. time. Recent particle tracking results using the coupled $\psi(\mathbf{s}, t)$ have exhibited this same type of behavior [9].

In Sect. 2 we review the development of the CTRW pde for the coupled mode $\psi(\mathbf{s}, t)$. We focus on the problem of particles migrating in the complex flow field of a water-saturated geological formation, which is heterogeneous at multiple spatial scales. The transitions consist of a displacement $\mathbf{s}$ and velocity $v$ chosen from $\psi(\mathbf{s}, t)$ where $v = s/t$. Special attention is paid to obtaining analytic forms for the Laplace Transform of $\psi(\mathbf{s}, t)$. The spatial moments of the latter $\tilde{\psi}(\mathbf{s}, u)$, where $u$ is the Laplace variable, are numerically determined and inserted into the coupled CTRW pde. The numerical solution involves the inverse Laplace Transform, which is a difficult step and accomplished here for the first time with a coupled $\psi(\mathbf{s}, t)$. The results for the particle concentration $c(\mathbf{s}, t)$ are used to calculate breakthrough curves. In Sect. 3 we show the breakthrough curves as a function of the parameters determining $\psi(\mathbf{s}, t)$ and the flow conditions, and observe all the features associated with the quantitative changes in chemical plume propagation. The particle tracking results of [9] have exhibited similar dependencies of the parameters of $\psi(\mathbf{s}, t)$.

## 2 Coupled Transport Equation

There are a number of approaches that have been used to calculate transport properties of disordered systems. If there is sufficient characterization of the system one can solve a standard transport equation, the Master Equation,

$$\frac{\partial C(\mathbf{s}, t)}{\partial t} = -\sum_{\mathbf{s}'} w(\mathbf{s}', \mathbf{s}) C(\mathbf{s}, t) + \sum_{\mathbf{s}'} w(\mathbf{s}, \mathbf{s}') C(\mathbf{s}', t) \tag{1}$$

for $C(\mathbf{s}, t)$, the normalized particle density, for a single realization of the system. The solution of (1) depends on the site distribution $\{\mathbf{s}\}$ and the transitions between them $w(\mathbf{s}, \mathbf{s}')$. The result can subsequently be averaged over an ensemble of system configurations [14]. If the system is highly heterogeneous and not well characterized, as are geological formations, another approach is to ensemble average the Master Equation and determine a Generalized Master Equation (GME) [15, 23]

$$\frac{\partial c(\mathbf{s}, t)}{\partial t} = -\sum_{\mathbf{s}'} \int_0^t \phi(\mathbf{s}' - \mathbf{s}, t - t') c(\mathbf{s}, t') dt' + \sum_{\mathbf{s}'} \int_0^t \phi(\mathbf{s} - \mathbf{s}', t - t') c(\mathbf{s}', t') dt'. \tag{2}$$

The GME is equivalent to a continuous time random walk (CTRW) with the relationship (in Laplace space)

$$\tilde{\phi}(\mathbf{s}, u) = \frac{u \tilde{\psi}(\mathbf{s}, u)}{1 - \tilde{\psi}(u)}, \qquad \tilde{\psi}(u) = \sum_{\mathbf{s}} \tilde{\psi}(\mathbf{s}, u) \tag{3}$$

where $\tilde{f}(u)$ denotes the Laplace transform (LT) of $f(t)$; using LT and a discrete Fourier Transform the formal solution of (2) in the form of a coupled CTRW on a lattice with periodic boundary conditions is contained in [22]. The asymptotic behavior of this solution

was explored in [24]. The pdf $\psi(\mathbf{s}, t)$ is generated by the spectrum of transitions $w(\mathbf{s}, \mathbf{s}')$ of the system (details in [23]).

The next step in deriving the CTRW pde transport equation is the expansion of $c(\mathbf{s}', t)$ in the GME (2) [4]

$$c(\mathbf{s}', t) \approx c(\mathbf{s}, t) + (\mathbf{s}' - \mathbf{s}) \cdot \nabla c(\mathbf{s}, t) + \frac{1}{2}(\mathbf{s}' - \mathbf{s})(\mathbf{s}' - \mathbf{s}) : \nabla\nabla c(\mathbf{s}, t) \tag{4}$$

with the dyadic symbol : denoting a tensor product.

The insertion of (4) into the GME (2) yields, in Laplace space [3, 8]

$$u\tilde{c}(\mathbf{s}, u) - c_0(\mathbf{s}) = -\mathbf{v}^*(u) \cdot \nabla\tilde{c}(\mathbf{s}, u) + \mathbf{D}^*(u) : \nabla\nabla\tilde{c}(\mathbf{s}, u) \tag{5}$$

where we define an advective component

$$\mathbf{v}^*(u) \equiv \int \tilde{\phi}(\mathbf{s}, u)\mathbf{s}d\mathbf{s} = u\frac{\int \tilde{\psi}(\mathbf{s}, u)\mathbf{s}d\mathbf{s}}{1 - \tilde{\psi}(u)} \tag{6}$$

and a dispersive component

$$\mathbf{D}^*(u) \equiv \frac{1}{2}\int \tilde{\phi}(\mathbf{s}, u)\mathbf{s}\mathbf{s}d\mathbf{s} = \frac{u}{2}\frac{\int \tilde{\psi}(\mathbf{s}, u)\mathbf{s}\mathbf{s}d\mathbf{s}}{1 - \tilde{\psi}(u)}. \tag{7}$$

Observe that the GME does not separate the transport into advective and dispersive components of the motion. Here, too, the separation is only apparent. In fact, the $u$-dependence of (6) and (7) indicates that the nonlocality in time (cf. discussion following (26) in [4]) applies to both the advective and dispersive parts of the motion, where $\mathbf{v}^*(u)$ and $\mathbf{D}^*(u)$ are different spatial moments of the same distribution $\tilde{\phi}(\mathbf{s}, u)$ and are hence connected.

It has been shown that the approximation of using a decoupled form $\psi(\mathbf{s}, t) = p(\mathbf{s})\psi(t)$ is effective for a compact distribution of displacements [9]. A departure in the properties of plume propagation (a pulse of particles) occurs for a broad distribution of $s$ (a power law as in a Lévy distribution). The enhanced transport behavior of both an algebraic dependence of $s$ and $t$ of $\psi(\mathbf{s}, t)$ has been explored using particle tracking [9]. In this paper we explore for the first time the solutions of the fully coupled form of (5) and demonstrate an enhancement of transport behaviors over ones reported in the literature.

### 2.1 A Model of Coupled Propagation

Each transition consists of a choice of displacement $\mathbf{s}$ with a distribution $F(\mathbf{s})$ and one in velocity (determined by the steady state flow field) $\Phi(\xi)$ (where $\xi = 1/v$, $v$ = velocity). The distributions are each normalized. The space-time coupling is through the velocity $t = s\xi$:

$$\psi(\mathbf{s}, t) = F(\mathbf{s})\frac{\Phi(t/s)}{s} \tag{8}$$

where we use the relation $\delta(s\xi - t) = \delta(\xi - \frac{t}{s})/s$. For $F(\mathbf{s})$ we use a product form for the angular variable

$$F(\mathbf{s})d\mathbf{s} = s^{d-1}p(s)ds\Omega(\boldsymbol{\omega})d\boldsymbol{\omega} \tag{9}$$

where the angle vector $\boldsymbol{\omega}$ is distributed according to $\Omega(\boldsymbol{\omega})$. The spatial moments of $\psi(\mathbf{s}, t)$ are

$$\mu_i^{(1)}(t) = a_i\mu^{(1)}(t), \qquad \mu_{ij}^{(2)} = b_{ij}\mu^{(2)}(t) \tag{10}$$

where

$$\mu^{(\iota)}(t) = \int_0^\infty \mathrm{d}s s^{d-2} s^\iota p(s) \Phi(t/s) \tag{11}$$

and

$$a_i = \int \mathrm{d}\boldsymbol{\omega} \Omega(\boldsymbol{\omega}) f_i(\boldsymbol{\omega}), \qquad b_{ij} = \int \mathrm{d}\boldsymbol{\omega} \Omega(\boldsymbol{\omega}) f_i(\boldsymbol{\omega}) f_j(\boldsymbol{\omega}). \tag{12}$$

The $f_i(\boldsymbol{\omega})$ are the direction functions (for $d = 2$ dimensions, $f_1(\omega) = \cos(\omega)$ and $f_2(\omega) = \sin(\omega)$).

We present expressions using the latter forms but all our simulation results here are performed in 2d domains. For the 2d case we use two normalized versions of $\Omega(\omega)$: a uniform distribution

$$\Omega_u(\omega) = \frac{2}{\pi} \Theta\left(\frac{\pi^2}{16} - \omega^2\right) \tag{13}$$

and a normal distribution

$$\Omega_n(\omega) = \exp(-\omega^2/2\sigma_n^2)/\sigma_n\sqrt{2\pi} \tag{14}$$

where $\Theta(\chi)$ is the Heaviside function. Using (13), (14) respectively, $a_i = \delta_{i1}[2\sqrt{2}/\pi$, $\exp(-\sigma_n^2/2)]$ and $b_{ij} = \delta_{ij} b_i$, $b_{3/2\mp 1/2} = [1/2 \pm 1/\pi, 1/2 \pm \exp(-2\sigma_n^2)/2]$.

For $p(s)$ in (9) we focus on a Lévy-like distribution

$$p(s') = C_s \frac{\exp(-s'/\lambda_2)}{(s_1' + s')^{1+\alpha}}. \tag{15}$$

Using the same functional notation but with a dimensionless spatial displacement (with a normalization constant $C_s$ defined in this form), we have

$$p(s) = \frac{\exp(-s/s_2)}{(s_1')^2 \mathcal{I} (1+s)^{1+\alpha}} \tag{16}$$

with $s = s'/s_1'$ and $s_2 = \lambda_2/s_1'$ and

$$\mathcal{I} = \int_0^\infty \mathrm{d}s e^{-s/s_2} \frac{s}{(1+s)^{1+\alpha}} = s_2^{1-\alpha} \exp(1/s_2) \left[\Gamma(1-\alpha, 1/s_2) - \frac{1}{s_2}\Gamma(-\alpha, 1/s_2)\right], \tag{17}$$

where $\Gamma(a, x)$ is the incomplete gamma function formula 6.5.3 in [1].

The velocity distribution is

$$\Phi(\xi) = C_\xi \Upsilon(\xi) \frac{\exp(-\xi/\lambda_1)}{(c_\xi + \xi)^{1+\beta}} \tag{18}$$

where we use for $\Upsilon(\xi)$ governing the high velocity or low $\xi$ behavior,

$$\Upsilon(\xi) = \exp(-\xi_0/\xi), \tag{19}$$

where $C_\xi$ is the appropriate normalization constant, $c_\xi$ is a constant and $\lambda_1$ is a cut-off. The forms for $\Phi(\xi)$ in (18) and (19) are chosen to provide flexibility in the character of the velocity spectrum. The high $\xi$ dependence has the form of a truncated power-law, which gives

rise to a power-law time dependence associated with non-Fickian transport [8]. In order to minimize the extent of the numerical work in the solution of the pde (5) we specialize the parameters in (18) and (19):

$$\Phi(\xi) = C_\xi \exp(-\xi_0/\xi)\exp(-\xi/\lambda_1)\xi^{-1-\beta}. \tag{20}$$

We set $c_\xi = 0$; the parameter $c_\xi$ plays the role of a scale factor but is not needed in (18) as $\xi_0$ can play that role. The values of $\beta$, which determine the extent of the power-law dependence, are chosen to be restricted to $\beta = 1/2, 3/2$ in order to obtain an analytic Laplace transform of (18) ($t = s\xi$). These values of $\beta$ correspond to different regimes of dispersion. The particle tracking results in [9] have been obtained in these regimes. The normalized forms are

$$\Phi(t/s')/s' = \frac{\exp(-\chi/2t - t/\tau + (2\chi/\tau)^{1/2})}{\chi(2\pi)^{1/2}}\left(\frac{\chi}{t}\right)^{3/2}, \quad \beta = 1/2, \tag{21}$$

$$\Phi(t/s')/s' = \frac{\exp(-\chi/2t - t/\tau + (2\chi/\tau)^{1/2})}{\chi(2\pi)^{1/2}((2\chi/\tau)^{1/2}+1)}\left(\frac{\chi}{t}\right)^{5/2}, \quad \beta = 3/2 \tag{22}$$

with $\chi = 2st_1, t_1 = s_1'\xi_0, \tau = st_2 = ss_1'\lambda_1$.

The Laplace Transform of $\Phi(t/s')/s'$ is

$$\tilde{\Phi}(u)/s' = \exp(-(2\chi u + 2\chi/\tau)^{1/2} + (2\chi/\tau)^{1/2}), \quad \beta = 1/2, \tag{23}$$

$$\tilde{\Phi}(u)/s' = e^{-(2\chi u + 2\frac{\chi}{\tau})^{1/2} + (2\frac{\chi}{\tau})^{1/2}}\frac{(2\chi u + 2\frac{\chi}{\tau})^{1/2}+1}{(2\frac{\chi}{\tau})^{1/2}+1}, \quad \beta = 3/2. \tag{24}$$

## 2.2 Integrals for Spatial Moments of $\tilde{\psi}(\mathbf{s}', u)$

The moments that enter (6) and (7) are, using (16) for $p(s)$ and setting for typesetting convenience $r(s,u) = 2(\frac{t_1}{t_2})^{1/2}(1-(st_2u+1)^{1/2})$

$$\tilde{\mu}^{(\iota)}(u) = \frac{(s_1')^\iota}{s_2^{1-\alpha}\mathcal{I}^*}\int_0^\infty \mathrm{d}s \frac{s^{1+\iota}e^{-s/s_2}}{(1+s)^{1+\alpha}}\exp(r(s,u)), \quad \beta = 1/2 \tag{25}$$

and

$$\tilde{\mu}^{(\iota)}(u) = \frac{(s_1')^\iota}{s_2^{1-\alpha}\mathcal{I}^*}\int_0^\infty \mathrm{d}s \frac{s^{1+\iota}e^{-s/s_2}}{(1+s)^{1+\alpha}}\left[1 - \frac{r(s,u))}{2(\frac{t_1}{t_2})^{1/2}+1}\right]\exp(r(s,u)), \quad \beta = 3/2 \tag{26}$$

with

$$\mathcal{I}^* \equiv s_2^{-1+\alpha}\int_0^\infty \mathrm{d}s \frac{s\,e^{-s/s_2}}{(1+s)^{1+\alpha}} = e^{1/s_2}\left[\Gamma\left(1-\alpha, \frac{1}{s_2}\right) - \frac{1}{s_2}\Gamma\left(-\alpha, \frac{1}{s_2}\right)\right]. \tag{27}$$

The moments $\tilde{\mu}^{(\iota)}(u)$ determine the $u$-dependent coefficients of the pde in Laplace space. We change the variable $s = xs_2$ with the result

$$\tilde{\mu}^{(\iota)}(u) = \frac{(s_1's_2)^\iota}{\mathcal{I}^*}\int_0^\infty \mathrm{d}x x^{1+\iota}\frac{e^{-x}}{(\frac{1}{s_2}+x)^{1+\alpha}}\exp(r(xs_2,u)) \tag{28}$$

and

$$\tilde{\mu}^{(\iota)}(u) = \frac{(s_1' s_2)^\iota}{\mathcal{I}^*} \int_0^\infty \mathrm{d}x \frac{x^{1+\iota}\, e^{-x}}{(\frac{1}{s_2}+x)^{1+\alpha}} \left[1 - \frac{r(xs_2,u))}{2(\frac{t_1}{t_2})^{1/2}+1}\right] \exp(r(xs_2,u)) \tag{29}$$

for $\beta = 1/2$ and $3/2$, respectively. It is numerically convenient to use

$$1 - \tilde{\mu}^0(u) = \frac{1}{\mathcal{I}^*} \int_0^\infty \mathrm{d}x x \frac{e^{-x}}{(\frac{1}{s_2}+x)^{1+\alpha}} [1 - \exp(r(xs_2,u))] \tag{30}$$

and

$$1 - \tilde{\mu}^0(u) = \frac{1}{\mathcal{I}^*} \int_0^\infty \mathrm{d}x \frac{x\, e^{-x}}{(\frac{1}{s_2}+x)^{1+\alpha}} \left\{1 - \left[1 - \frac{r(xs_2,u))}{2(\frac{t_1}{t_2})^{1/2}+1}\right] \exp(r(xs_2,u))\right\} \tag{31}$$

for $\beta = 1/2$ and $3/2$, respectively, for the zeroth moment in (6), (7). In the other expressions $\iota = 1, 2$. The moments $\tilde{\mu}^{(\iota)}(u)$ determine the $u$-dependent coefficients of the pde in Laplace space (5).

The parameter controlling the $u \to 0$ limit is the reciprocal of $s_2 t_2$, and $s_2$ controls the magnitude of the exponent in the integrals so we cannot make $s_2$ too large. We will typically use $s_2 = 10^4$, $t_2 = 10^4$, $10^5$, and $\alpha = 1.8, 2.5$.

We note that the expressions (28), (29) for $\tilde{\mu}^{(\iota)}(u) \iota = 1, 2$ and (30), (31) for $1 - \tilde{\mu}^0(u)$ have a common factor $\frac{1}{\mathcal{I}^*}$. Hence inserting these expressions into (6) and (7),

$$v_i^*(u) = a_i t^* u v \frac{s_2 \int_0^\infty \mathrm{d}x \frac{x^2 e^{-x}}{(\frac{1}{s_2}+x)^{1+\alpha}} \exp(r(xs_2,u))}{\int_0^\infty \mathrm{d}x \frac{x\, e^{-x}}{(\frac{1}{s_2}+x)^{1+\alpha}} [1 - \exp(r(xs_2,u))]} \tag{32}$$

and

$$D_{ij}^*(u) = \frac{b_{ij} t^* u v \alpha_D s_2^2 \int_0^\infty \mathrm{d}x \frac{x^3 e^{-x}}{(\frac{1}{s_2}+x)^{1+\alpha}} \exp(r(xs_2,u))}{2 \int_0^\infty \mathrm{d}x \frac{x\, e^{-x}}{(\frac{1}{s_2}+x)^{1+\alpha}} [1 - \exp(r(xs_2,u))]} \tag{33}$$

for $\beta = 1/2$, and

$$v_i^*(u) = a_i t^* u v \frac{s_2 \int_0^\infty \mathrm{d}x \frac{x^2 e^{-x}}{(\frac{1}{s_2}+x)^{1+\alpha}} [1 - \frac{r(xs_2,u))}{2(\frac{t_1}{t_2})^{1/2}+1}] \exp(r(xs_2,u))}{\int_0^\infty \mathrm{d}x \frac{x\, e^{-x}}{(\frac{1}{s_2}+x)^{1+\alpha}} \{1 - [1 - \frac{r(xs_2,u))}{2(\frac{t_1}{t_2})^{1/2}+1}] \exp(r(xs_2,u))\}} \tag{34}$$

and

$$D_{ij}^*(u) = \frac{b_{ij} t^* u v \alpha_D s_2^2 \int_0^\infty \mathrm{d}x \frac{x^3 e^{-x}}{(\frac{1}{s_2}+x)^{1+\alpha}} [1 - \frac{r(xs_2,u))}{2(\frac{t_1}{t_2})^{1/2}+1}] \exp(r(xs_2,u))}{2 \int_0^\infty \mathrm{d}x \frac{x\, e^{-x}}{(\frac{1}{s_2}+x)^{1+\alpha}} \{1 - [1 - \frac{r(xs_2,u))}{2(\frac{t_1}{t_2})^{1/2}+1}] \exp(r(xs_2,u))\}} \tag{35}$$

for $\beta = 3/2$, where $s_1'/t^* = v$ and $s_1'/t_1 = 1/\xi_0$ and $s_1' = \alpha_D$ (we usually set $t^* = t_1$).

We evaluate the integrals in (32), (34), (33) and (35) numerically using the Gaussian type formula 25.4.45 in [1]. Inserting the appropriate values of (13) or (14) into (32), (34), (33) and (35) we determine the coefficients in (5). The inverse Laplace Transform algorithm of *de Hoog et al.* [7] was employed to invert the numerical solution of (5) to obtain $c(\mathbf{s}, t)$. The

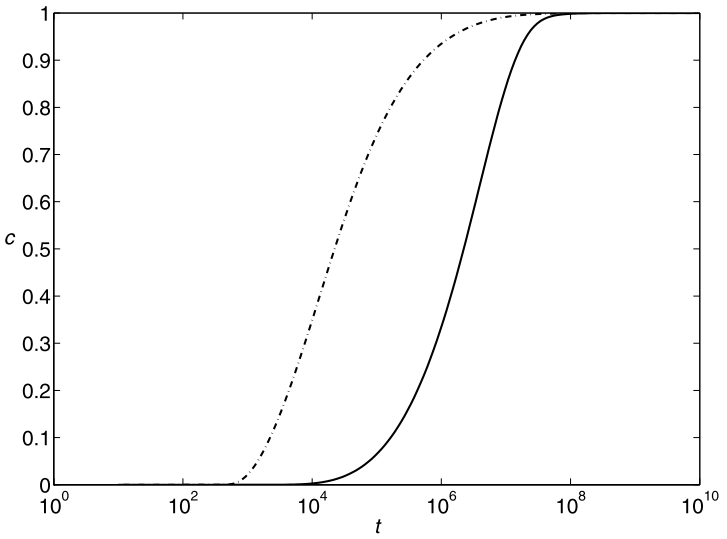


**Fig. 1** Breakthrough curves (step input) with the parameters $t_1 = 0.01$ s, $t_2 = 10^5$ s, $s_2 = 10^4$ cm, $\alpha_D = 0.05$ cm, $Q_{in} = 2$ ml/min, with $\beta = 1/2$ and $\alpha = 1.8$ (*dashed line*) and $\alpha = 2.5$ (*solid line*)

numerical stability of the Laplace inversion depends on the input parameters. The range of parameters we use provides a very useful set of solutions, which determine the breakthrough curves that we exhibit in Figs. 1–4 in Sect. 3.

## 3 Results and Discussion

In each of Figs. 1–3, the breakthrough curves correspond to a step input of normalized particle concentration and in Fig. 4 to a pulse input. For these figures the values chosen for the parameters are representative dimensions, $L = 25$ cm, $d = 2$ cm, porosity $n = 0.35$, diffusivity, $\alpha_D = 0.05$ cm and flow rate, $Q_{in} = 2$ ml/min. The parameters of the distribution pdf (16) and (21), (22) (with the subsequent definitions) are chosen to set the time scale and to allow a large region of power law dependence: $t_2 = 10^5$ s, $s_2 = 10^4$ cm. The variable parameters are $\beta, t_1, \alpha$.

In Figs. 1 and 2 we show the effects on the breakthrough curve of varying $\alpha$ for each of the $\beta$ values. In Fig. 1 the breakthrough curve is evaluated for the highly dispersive regime of $\beta = 1/2$ and hence the change in $\alpha$ from 1.8 to 2.5 (which leads to a more Gaussian-like distribution) produces a large shift. The earlier arrival of the $\alpha = 1.8$ relative to the $\alpha = 2.5$ is striking and is a key result. Similar change with $\alpha$ can be seen in Fig. 6 in [9]. The origin of this dependence can be seen in Fig. 4 in [9]. The enhanced transport due to a power law in displacements leads to a different mix of transitions. The earlier time large displacements clearly influence the broad tail due to the power law in time. The result is earlier arrivals for the larger dispersion in $s$ and hence the behavior as seen in Fig. 1. In Fig. 2 the breakthrough curve is in the less dispersive regime of $\beta = 3/2$ and the effect of varying $\alpha$ is reduced but the relative behavior is the same as in Fig. 1. Note that each of the breakthrough curves in Fig. 2 covers a much narrower range from arrival to saturation than those in Fig. 1. This is clearly shown in Fig. 3 for the two different $\beta$ values for a fixed value of $\alpha$. In Fig. 4 we vary

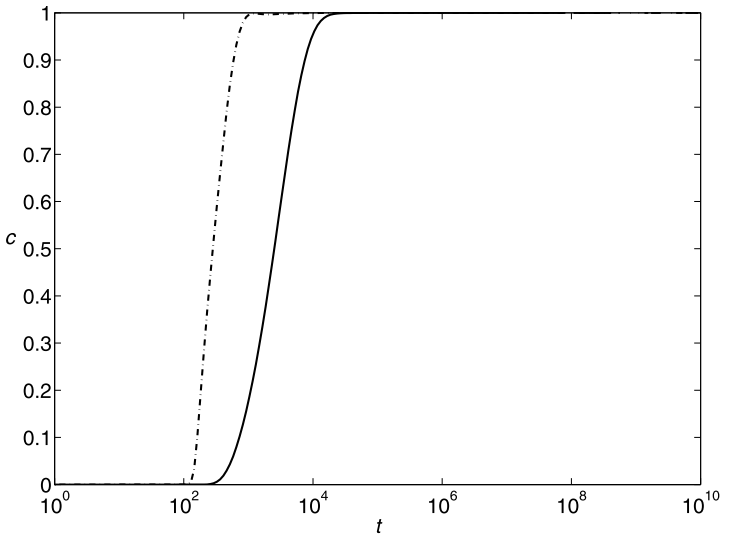


**Fig. 2** Breakthrough curves (step input) with the parameters $t_1 = 0.01$ s, $t_2 = 10^5$ s, $s_2 = 10^4$ cm, $\alpha_D = 0.05$ cm, $Q_{in} = 2$ ml/min, with $\beta = 3/2$ and $\alpha = 1.8$ (*dashed line*) and $\alpha = 2.5$ (*solid line*)

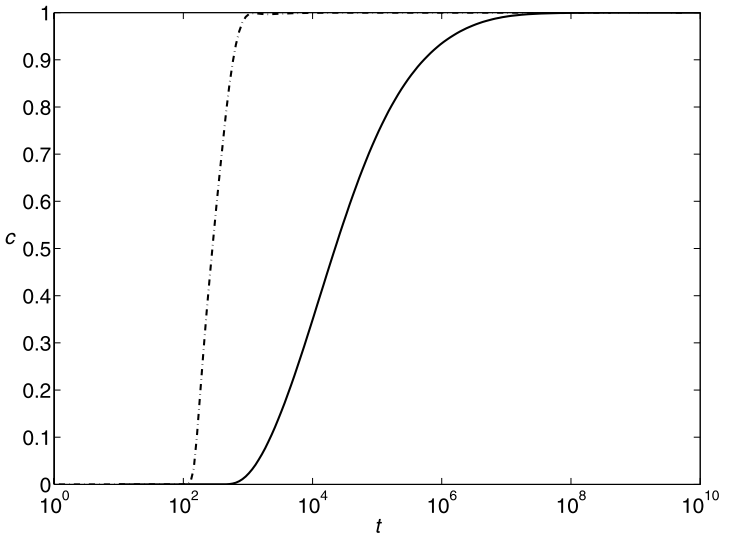


**Fig. 3** Breakthrough curves (step input) with the parameters $t_1 = 0.01$ s, $t_2 = 10^5$ s, $s_2 = 10^4$ cm, $\alpha_D = 0.05$ cm, $Q_{in} = 2$ ml/min, with $\alpha = 1.8$ and $\beta = 1/2$ (*solid line*) and $\beta = 3/2$ (*dashed line*)

$t_1$ and keep $t^*$ constant, i.e., this is equivalent to varying $\xi_0$ and the behavior mimics that of Fig. 7 in [9]. In the case when there is a higher proportion of higher velocities there is more opportunity in any time interval to allow larger displacements and hence earlier arrivals (the cutoff for the higher velocities is $v < 1/\xi_0$). The two breakthrough curves in Fig. 4 illustrate the subtlety of the coupled dynamics; with a fixed $\alpha$ and $\beta$ different results were obtained

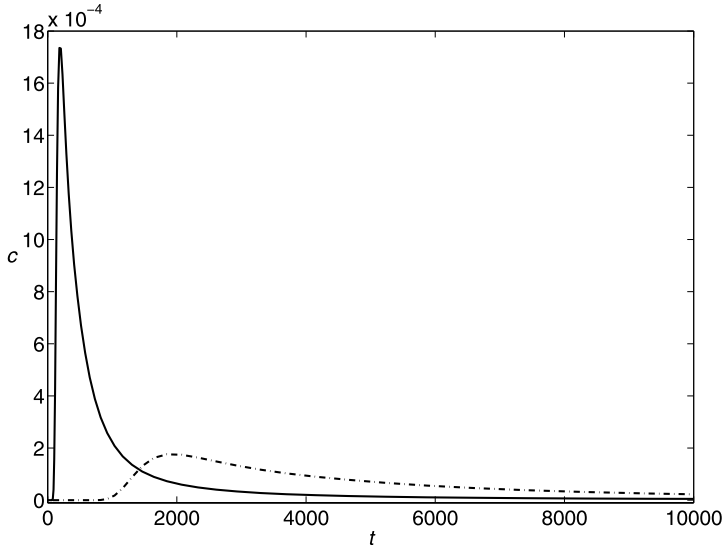


**Fig. 4** Breakthrough curves (pulse input, linear scale) with the parameters $t^* = 0.1$ s, $t_2 = 10^5$ s, $s_2 = 10^4$ cm, $\alpha_D = 0.05$ cm, $Q_{in} = 2$ ml/min, with $\alpha = 1.8$ and $\beta = 1/2$ and $t_1 = 0.01$ (*solid line*) and $t_1 = 0.1$ (*dashed line*)

by simply changing the proportion of the high velocity part of $\Phi(\xi)$. The solid curve has features that could distinguish it from the more dispersive decoupled breakthrough curves. It is highly abrupt and peaked in the early times while having a long time tail. However the dashed line does not have these features. In fitting experimental breakthrough curves, the need to use a coupled CTRW cannot be determined solely by a definitive breakthrough curve shape but rather by knowledge of the system structure (e.g., a random fracture network) and the values of the parameters (as compared to a fitting with a decoupled CTRW).

There is clearly an interplay between the power-laws in $s$ and $t$. In Fig. 1 the dashed line ($\alpha = 1.8$) has a total dispersion width of nearly four orders of magnitude while the width of the solid line ($\alpha = 2.5$) is close to three orders of magnitude. Even though in this regime of $\beta = 1/2$ the dispersion is dominated by the (power-law) $t$-dependence of $\psi(\mathbf{s}, t)$ the dispersion is enhanced by the extent of the power-law in $s$. In Fig. 2 in the $\beta = 3/2$ regime there is less overall dispersion and the effect of $\alpha$ is reduced (Fig. 3 shows the change in dispersion of a shift in $\beta$ values). As observed by all the results the coupled $\psi(\mathbf{s}, t)$ is sufficient to limit the large displacements of $p(s)$ (16) in each time range and provide convergence of the moments (25), (26). This is a crucial step in exhibiting the enriched plume propagation behavior of the coupled CTRW pde transport equation, which is the main result of this paper.

**Acknowledgements** The financial support of the European Commission (contract PITN-GA-2008-212298) is gratefully acknowledged.

## References

1. Abramowitz, M., Stegun, I.: Handbook of Mathematical Functions. Dover Publications, Inc., New York (1970)

2. Berkowitz, B., Scher, H.: Theory of anomalous chemical transport in fracture networks. Phys. Rev. E **57**(5), 5858–5869 (1998)
3. Berkowitz, B., Klafter, J., Metzler, R., Scher, H.: Physical pictures of transport in heterogeneous media: advection-dispersion, random walk and fractional derivative formulations. Water Resour. Res. **38**(10), 1191 (2002). doi:10.1029/2001WR001,030
4. Berkowitz, B., Cortis, A., Dentz, M., Scher, H.: Modeling non-Fickian transport in geological formations as a continuous time random walk. Rev. Geophys. **44**, RG2003 (2006). doi:10.1029/2005RG000,178
5. Bijeljic, B., Blunt, M.J.: Pore-scale modeling and continuous time random walk analysis of dispersion in porous media. Water Resour. Res. **42**, W01,202 (2006). doi:10.1029/2005WR004,578
6. Bouchaud, J.P., Georges, A.: Anomalous diffusion in disordered media: Statistical mechanisms, models and physical applications. Phys. Rep. **195**, 127–293 (1990)
7. de Hoog, F.R., Knight, J.H., Stokes, A.N.: An improved method for numerical inversion of Laplace transforms. SIAM J. Sci. Stat. Comput. **3**, 357–366 (1982)
8. Dentz, M., Cortis, A., Scher, H., Berkowitz, B.: Time behavior of solute transport in heterogeneous media: transition from anomalous to normal transport. Adv. Water Resour. **27**(2), 155–173 (2004). doi:10.1016/j.advwatres.2003.11.002
9. Dentz, M., Scher, H., Holder, D., Berkowitz, B.: Transport behavior of coupled continuous time random walks. Phys. Rev. E **78** (2008). doi:10.1103,041,110
10. Di Donato, G., Obi, E.O., Blunt, M.J.: Anomalous transport in heterogeneous media demonstrated by streamline-based simulation. Geophys. Res. Lett. **30**, 1608–1612 (2003). doi:10.1029/2003GL017,196
11. Eggleston, J., Rojstaczer, S.: Identification of large-scale hydraulic conductivity trends and the influence of trends on contaminant transport. Water Resour. Res. **34**(9), 2155–2168 (1998)
12. Fiori, A., Janković, I., Dagan, G., Cvetković, V.: Ergodic transport through aquifers of non-Gaussian log-conductivity distribution and occurrence of anomalous behavior. Water Resour. Res. **43**, W07,445 (2007). doi:10.1029/2007WR005,976
13. Gelhar, L.W.: Stochastic Subsurface Hydrology. Prentice Hall, Englewood Cliffs (1993)
14. Holder, D., Scher, H., Berkowitz, B.: Numerical study of diffusion on a random-mixed-bond lattice. Phys. Rev. E **77**, 031119 (2008). doi:10.1103/PhysRevE.77.031119
15. Klafter, J., Silbey, R.: Derivation of continuous-time random walk equations. Phys. Rev. A **44**(2), 55–58 (1980)
16. Klafter, J., Blumen, A., Shlesinger, M.F.: Stochastic pathway to anomalous diffusion. Phys. Rev. A **35**(7), 3081–3085 (1987)
17. Lallemand-Barres, P., Peaudecerf, P.: Recherche des relations entre valeur de la dispersivité macroscopique d'un aquifére, ses autres caractéristiques et les conditions de mesure. Bull. Bur. Rech. Geol. Min. Fr. (Sect. 3) **4**, 277–284 (1978)
18. Levitz, P.: The Pareto-Levy law and the distribution of income. Europhys. Lett. **39**, 593 (1997)
19. Lévy, P.: Théorie de l'Addition des Variables Alé atoires. Gauthier Villars, Paris (1937)
20. Mandelbrot, B.B.: From Knudsen diffusion to Levy walk. Int. Econ. Rev. **1**, 79 (1960)
21. Metzler, R., Klafter, J.: The random walk's guide to anomalous diffusion: a fractional dynamics approach. Phys. Rep. **339**(1), 1–77 (2000)
22. Scher, H., Lax, M.: Stochastic transport in a disordered solid. I. Theory. Phys. Rev. B **7**(1), 4491–4502 (1973)
23. Scher, H., Willbrand, K., Berkowitz, B.: Transport in disordered media with spatially nonuniform fields. Phys. Rev. E **81**, 031102 (2010). doi:10.1103/PhysRevE.81.031102
24. Shlesinger, M.F., Klafter, J., Wong, Y.M.: Random walks with infinite spatial and temporal moments. J. Stat. Phys. **27**(3), 499–512 (1982)
25. Tyutnev, A.P., Saenko, V.S., Pozhidaev, E.D., Kolesnikov, V.: Verification of the dispersive charge transport in a hydrazone:polycarbonate molecularly doped polymer. J. Phys., Condens. Matter **21**, 115107 (2009)
26. Zhang, X., Lv, M.: Persistence of anomalous dispersion in uniform porous media demonstrated by pore-scale simulations. Water Resour. Res. **43**, W07,437 (2007)